ELSEVIER

Materials Science and Engineering A257 (1998) 322–327

MATERIALS SCIENCE & ENGINEERING A

Laser shock processing of 2024-T62 aluminum alloy

Zhang Hong [a,*], Yu Chengye [b]

[a] *Department of Mechanical Engineering, Changchun Institute of Optics and Fine Mechanics, No.7 Weixing Road, Changchun, 130022, People's Republic of China*

[b] *Department of Mechanical Engineering, Nanjing University of Aeronautics and Astronautics, No.29 Yudao Street, Nanjing, 210016, People's Republic of China*

Received 11 March 1998; received in revised form 24 June 1998

Abstract

Laser shock processing (LSP) is a relatively new technique for strengthening metals. A method developed for optimizing the LSP parameters is reported in this paper. The effects of LSP on the microstructure, hardness, surface roughness, residual stress, fatigue life, fatigue crack growth (FCG) of 2024-T62 aluminum alloy were investigated. The fatigue life of the laser-shocked specimens was two times greater than that of the unshocked specimens. The fatigue crack growth rates (FCGRs) at a given stress intensity were reduced by over one order of magnitude. The fatigue behavior improvements were attributed to a combination of increased dislocation density, decreased surface roughness and compressive residual stress induced by the laser shock waves.

Keywords: Laser shock processing; Aluminum alloy; Fatigue; Fatigue crack growth

1. Introduction

The feasibility of using laser-induced shock waves to modify material properties and microstructures has been demonstrated by many studies [1–10]. In the laser shock process, a sacrificial material (such as black paint) is usually used as surface coating. While a high power, short laser pulse is focused on the surface, a plasma can be produced due to the melting and vaporizing of the surface coating. As this plasma expands, an intense shock wave propagates into the metal. While the pressure of the shock wave exceeds the dynamic yield strength of the metal, plastic deformation will occur causing modification of the near-surface microstructure and properties. In order to obtain the required pressure, a transparent overlay is used to confine the plasma expansion [11–16].

The aim of this paper is to describe a method developed for optimizing the LSP parameters and to study the effects of LSP on the mechanical properties and microstructures of 2024-T62 aluminum alloy.

2. Pressure produced by LSP

Based upon the hypotheses of Fabbro et al [17], two important factors which affect the pressure have been taken into account in our study [18]. One is the absorption coefficient of the surface coating, A. Another is the transmission coefficient of the transparent overlay, M. Thus, the pressure can be expressed as following:

$$P = 0.25\sqrt{I_0\, MAZ} \tag{1}$$

where P is the pressure induced by the laser-shock wave, I_0 is the laser power density, and Z is the reduced shock impedance between the metal and the transparent overlay. Here P is expressed in bar, Z in kg m^{-2}s, and I_0 in W m^{-2}.

It is important to note that the pressure is proportional to the square root of the absorption coefficient of the surface coating and the transmission coefficient of the transparent overlay.

3. Optimization of LSP parameters

In the laser shock process, the LSP variable parameters include the laser power density, the spot size, and

* Corresponding author. Tel.: +86 431 5383466; fax: +86 431 5383815.

0921-5093/98/$ - see front matter
PII S0921-5093(98)00793-X

the pulse width. The relationship between these is given by:

$$E = \frac{\pi D^2}{4} I_0 \tau \quad (2)$$

where E is the laser pulse energy, D is the spot size, I_0 is the laser power density, and τ is the pulse width.

Optimization of the LSP parameters refers to optimization of the laser power density, spot size, and pulse width.

3.1. Optimization of laser power density

In order to obtain the deformation at the metal surface, the pressure induced by LSP should exceed the dynamic yield strength of the metal, σ_Y^D. Therefore, we have

$$P > 2\sigma_Y^D \quad (3)$$

From Eqs. (1) and (3), the minimum laser power density required by LSP can be expressed as:

$$I_{0\,\min} = \frac{64(\sigma_Y^D)^2}{MZA} \quad (4)$$

On the other hand, in order to prevent spalling at the rear face of metals, the pressure should not exceed the dynamic ultimate tensile strength of the metal, σ_U^D. So we have

$$P < 2\sigma_U^D \quad (5)$$

From Eqs. (1) and (5), the maximum laser power density needed by LSP can be written:

$$I_{0\,\min} = \frac{64(\sigma_U^D)^2}{MZA} \quad (6)$$

So the range of laser power density needed in laser shocking can be described as:

$$\frac{64(\sigma_Y^D)^2}{MZA} < I_0 < \frac{64(\sigma_U^D)^2}{MZA} \quad (7)$$

3.2. Optimization of spot size

We study the optimization of the spot size while considering a plate loaded in tension which contains a centrally located hole. The hole causes stress concentration. The stress at the edge of the hole is maximum. With the distance from the center increasing, the stress decreases. While the distance is three times of the hole radius, the stress decreases to the normal stress [19]. Therefore, in order to minimize the effect of stress concentration on the fatigue behavior and strengthen the circular hole, the spot size should be three times the diameter of the hole. Thus, we obtain

$$D = 3\,d \quad (8)$$

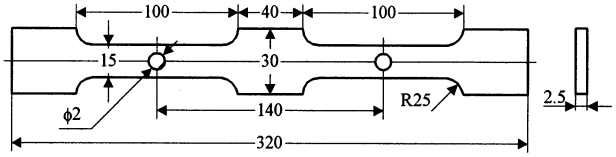

Fig. 1. Specimen shape used for fatigue tests (dimensions in mm).

here d is the diameter of the ready-shocked hole.

3.3. Optimization of pulse width

In order to obtain greater laser-shock processed depth, longer pulse width should be used [9]. However, ablation will occur if the pulse width is too long [20]. So the pulse width should be in the range from several nanoseconds to several tens of nanoseconds.

4. Experimental procedure

4.1. Material

The 2024-T62 material was received as 2.5 mm thick plate. The T62 condition consists of a solution treatment and natural aging. Its chemical compositions (wt.%) were: 0.5Si, 0.5Fe, 3.8Cu, 0.3Mn, 0.1Cr, 0.25Zn, 0.15Ti, balance Al. The mechanical properties were as follows: yield strength (0.2% offset) of 340 MPa, ultimate tensile strength of 425 MPa, elongation of 5%, and elastic modulus of 68.9 GPa.

The specimens used for the fatigue tests were of dog-bone type bi-detail structure, its shape was shown in Fig. 1. In order to compare the fatigue life of laser-shocked specimen with that of unshocked one in one operation on a single specimen, one hole was laser-shocked, the other was unshocked.

Center crack tension (CCT) specimens were used for the FCG tests, its shape was shown in Fig. 2. A 20 mm crack starter was made by electrical discharge wire machining, a fatigue crack starter was then initiated by cyclic loading of the specimen. Prior to measuring FCG, the tip of the fatigue crack was laser-shocked.

All fatigue and FCG tests specimens were machined with the loading axis parallel to the hot rolling direction (L).

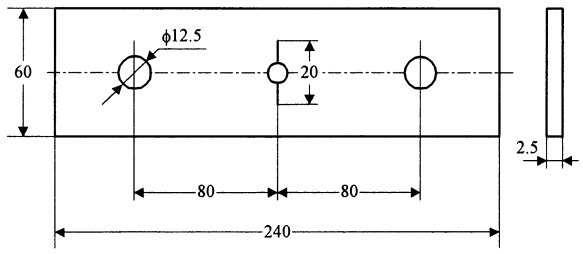

Fig. 2. Specimen shape used for FCG tests (dimensions in mm).

Table 1
Laser shocking parameters

Specimen types	I_0 (GW cm^{-2})	D (mm)	τ (ns)
Fatigue	1.57	6	18
FCG	7.32	8	23

4.2. Laser shock processing

The LSP experiments were performed using a Q-switched neodymium glass laser with a repetition rate of one cycle per minute and a wavelength of 1.06 μm.

These experiments were conducted using a confined plasma configuration at atmospheric pressure and room temperature. A 4.5 mm thick K7 glass was set on the specimen surface to confine the plasma. A 0.1 mm thick layer of black paint was placed between the glass and the specimen to enhance laser coupling and to protect the specimen surface from melting and vaporizing. Both sides of the specimen were shocked separately.

Using the relationships described in Section 3, the LSP parameters chosen for treating the fatigue and FCG specimens are shown in Table 1.

4.3. Characterization of the effects induced by LSP

Microhardness measurement was made with 50-g load and 15-s hold time. Surface profilometry was used to examine the surface roughness.

The microstructures were observed in a H-800 transmission electron microscope (TEM). The surface residual stresses were measured using an X-ray diffractometer.

4.4. Fatigue and FCG tests

All fatigue and FCG tests were performed in the tension-tension mode on INSTRON 1341 at room temperature in the air. R (the ratio of the minimum to the maximum stress intensity) was maintained at 0.1, and a frequency of 14 Hz with a sine wave form was used in the experiments.

The fatigue specimens were tested at a maximum load of 1.42 kN. Fifteen specimens were fatigue tested.

For crack growth, laser-shocked specimen required higher K_{max} (the maximum stress intensity) as compared to unshocked one. The unshocked FCG specimen was tested at a maximum load of 3.0 kN. However, the laser-shocked was at 3.4 kN. Only one specimen in each condition was tested. Crack lengths were measured at a magnification of $\times 30$ using a traveling microscope, with a accuracy of symbol 177 ± 0.01 mm.

5. Results

5.1. Hardness

The microhardness profiles measured at the surface across the laser irradiated spot shown in Fig. 3 revealed a significant increase in hardness in the laser-shock-processed zones as compared to the base. The maximum value reached 140 HV, i.e. 48 HV higher than the unshocked materials (92 HV).

5.2. Surface roughness

The mean surface roughness (Ra) of specimens measured before LSP was 1.6 μm. After LSP, the surface roughness was reduced significantly. The variation of the surface roughness with the laser power density was shown in Fig. 4. Higher laser power density produces lower surface roughness.

5.3. Residual stress

The relation between the laser power density and the surface residual stresses was plotted in Fig. 5. The measured results show that higher laser power density can produce greater surface compressive residual stresses.

5.4. Microstructural observations

The TEM observations were given in Fig. 6. From this figure, we can see the dislocation density of 2024-T62 aluminum alloy has been increased greatly after LSP.

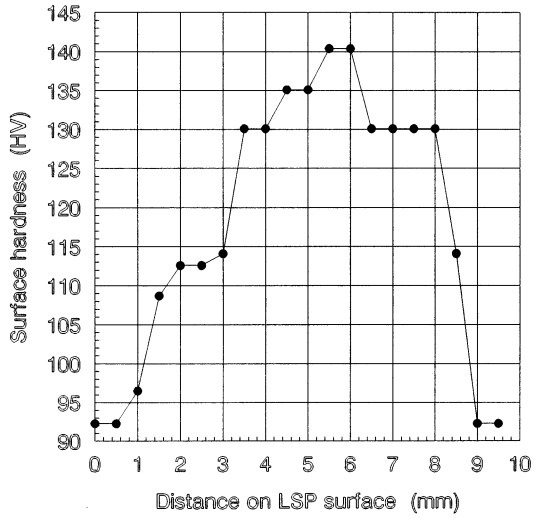

Fig. 3. Surface hardness profile across a laser irradiated spot ($E = 18$ J, $D = 8$ mm, $\tau = 23$ ns).

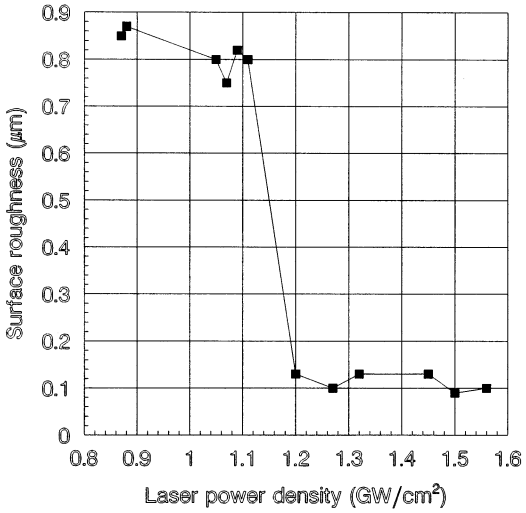

Fig. 4. Variations of the surface roughness with the laser power density ($D = 8$ mm, $\tau = 23$ ns).

5.5. Fatigue life

Fatigue tests results were shown in Table 2. We can see the fatigue life of 2024-T62 aluminum alloy after LSP was improved greatly. The laser-shocked specimens showed 2.2 times better fatigue lives on the average than the unshocked materials. However, the standard deviation of laser-shocked specimens was much more scatter than that of the unshocked specimens.

5.6. FCG

FCG data corresponding to unshocked and shocked specimens was in the form of FCGRs (da/dN) versus stress intensity factor range (ΔK).

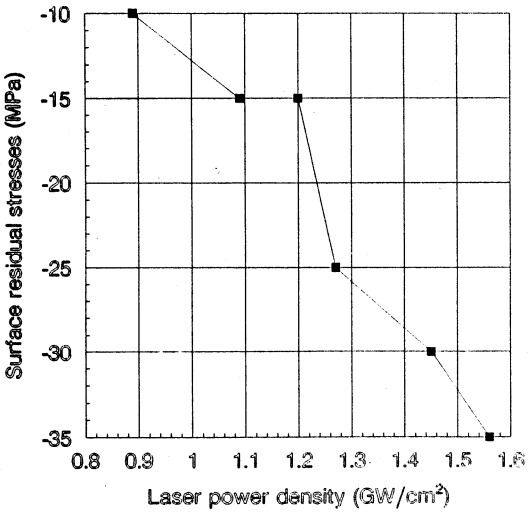

Fig. 5. Surface residual stress measurement as a function of the laser power density.

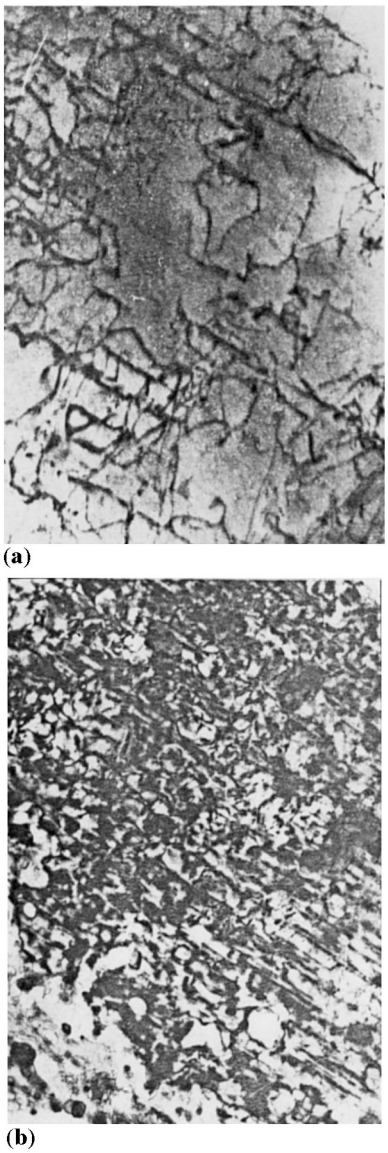

Fig. 6. Transmission electron micrographs of 2024-T62 aluminum alloy before and after laser shocking: (a), unshocked; (b), laser-shocked

To illustrate the effect of LSP, FCGRs data of laser-shocked specimen are compared in Fig. 7 with those of the unshocked condition. It is evident from Fig. 7 that laser shocking strongly influences FCG behavior. As a result of LSP, the FCGRs plot appears to be shifted to the right, corresponding to higher stress intensity factor range. A comparison of FCGRs at the same ΔK value shows a reduction of over one order of magnitude.

6. Discussion

The surface microhardness has been increased 50 percent after LSP of 2024-T62 aluminum alloy. Laser

Table 2
Fatigue life of 2024-T62 aluminum alloy

Specimen number	Unshocked	Laser-shocked
	No. of cycles to failure	No. of cycles to failure
1	66 010	127 210
2	86 390	186 880
3	69 990	121 130
4	73 970	158 620
5	86 700	186 420
6	72 320	166 980
7	82 430	174 480
8	63 670	237 230
9	68 700	245 400
10	78 810	148 140
11	67 030	129 970
12	62 690	122 470
13	74 600	161 750
14	87 950	130 850
15	90 830	211 680
Avg.	75 473	167 281
Std. dev.	9124	38 905

beam nonhomogeneity can be the cause of the scattered values of measured hardness. The increase in hardness after LSP can be attributed to the greater dislocation density indicated in our microstructural observations.

The increased dislocation density is characteristic of microstructural damage caused by the laser shock waves [21], which is beneficial to the improvement of fatigue life and the decrease of FCGRs.

As is known, a high surface roughness can generate local stress concentration which promote crack initiation. However, the surface roughness after LSP has been reduced significantly, which is may at least partially explain the observed improvement of fatigue crack initiation life.

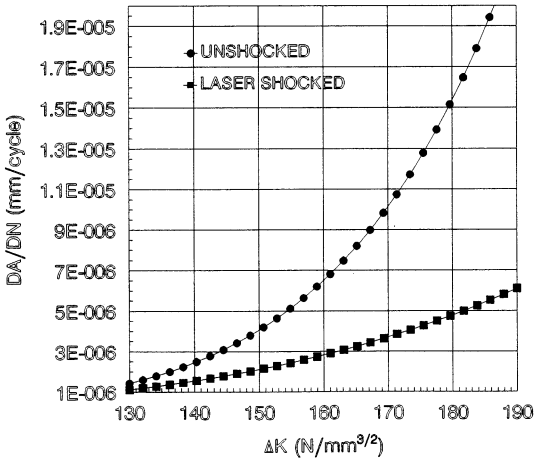

Fig. 7. Comparison of FCG in laser-shocked and unshocked conditions.

The increase in the fatigue life after LSP is a consequence of the compressive residual stresses introduced by the laser shock waves. Increased fatigue life with the introduction of the compressive residual stresses can be explained by the mean-stress effect [6].

The observed reduction in the FCGRs as a result of LSP can be understood by accounting for residual stresses induced by LSP. By applying the principle of superposition [22], the effective stress intensity factor, K_{eff}, can be defined as

$$K_{\text{eff}} = K_{\text{app}} + K_{\text{res}} \tag{9}$$

where K_{app} is the stress intensity caused by the applied load, and K_{res} is that caused by the residual stress.

In the presence of compressive residual stress, the $K_{\max}$ as well as $K_{\min}$ are reduced. The ΔK_{eff} ($\Delta K_{\text{eff}} = K_{\max} - K_{\min}$) that controls the FCGRs thus attains much lower levels as compared with ΔK_{eff} in the unshocked case, and thereby, leads to lower FCGRs.

7. Conclusions

In the laser-shock process, the optimization of the LSP parameters is essential, because it influences the shock conditions, and thereby influences the improvement of fatigue life and FCGRs. In this paper, a method for optimizing the LSP parameters has been proposed. In this method, the laser power density should be in the range from $64(\sigma_Y^D)^2/MZA$ to $64(\sigma_Y^D)^2/MZA$, the spot size should be three times that of the ready-shock hole diameter, and the pulse width should be from several nanoseconds to several tens of nanoseconds. By a series of fatigue tests, this method is proved to be practical.

The effects of LSP on 2024-T62 aluminum alloy have also been investigated. The fatigue tests results show that LSP can increase the fatigue life and decrease the FCGRs of 2024-T62 aluminum alloy, which results from the combinations of the surface compressive residual stress, reduced surface roughness, and increased dislocation density induced by the laser shock waves.

LSP is a promising and consistent method for strengthening aluminum alloys. With further study, LSP may find many industrial applications.

Acknowledgements

The authors would like to thank Professor Wu Hongxing and Senior Engineer Guo Dahao of the High Power Laser Laboratory at China University of Science and Technology for their help in performing the LSP experiments. We acknowledge the Aeronautical Industry Company of the People's Republic of China for the financial support.

References

[1] A.H. Clauer, B.P. Fairand, in: E.A. Metzbower (Ed.), Applications of Lasers in Materials Processing, American Society for Metals, Metals Park, Ohio, 1979, pp. 229–253.

[2] W.F. Bates, in: E.A. Metzbower (Ed.), Applications of lasers in Materials Processing, American Societty for Metals, Metals Park, Ohio, 1979, pp. 254–267.

[3] A.H. Clauer, C.T. Walters, S.C. Ford, in: E.A. Metzbower (Ed.), Applications of Lasers in Materials Processing, American Society for Metals, Metals Park, Ohio, 1983, pp. 7–22.

[4] A.H. Clauer, J.H. Holbrook, B.P. Fairand, in: M.A. Meyers, L.E. Murr (Eds.), Shock Waves and High-Strain-Rate Phenomena in Metals; Concepts and Applications, Plenum, New York, 1981, pp. 675–702.

[5] M. Gerland, M. Hallouin, H.N. Presles, Mater. Sci. Eng. A156 (1992) 175–182.

[6] G. Banas, H.E. Elsayed-Ali, F.V. Lawrence, J.M. Rigsbee, J. Appl. Phys. 67 (5) (1990) 2380–2384.

[7] J.P. Chu, J.M. Rigsbee, G. Banas, F.V. Lawrence, H.E. Elsayed-Ali, Metall. Trans. A 26A (1995) 1507–1517.

[8] B.P. Fairand, A.H. Clauer, in: S.D. Ferris, H.J. Lenoy, J.M. Poate (Eds.), Laser-Solid Interactions and Laser Processing, American Institute of Physics, New York, 1979, pp. 27–42.

[9] P. Peyre, R. Fabbro, P. Merrien, H.P. Lieurade, Mater. Sci. Eng. A210 (1996) 102–113.

[10] Zhang Hong, Lu Boliang, Zhang Shuren, Tang Yaxin, and Yu chengye, in: S.S.Deng and S.C.Wang (eds.), Laser Processing of Materials and Industrial Applications, SPIE 2888, Bellingham, 1996, 399–403.

[11] B.P. Fairand, A.H. Clauer, R.G. Jung, B.A. Wilcox, Appl. Phys. Lett. 25 (8) (1974) 431–433.

[12] N.C. Anderholm, Appl. Phys. Lett. 16 (3) (1970) 113–115.

[13] J.A. Fox, Appl. Phys. Lett. 24 (10) (1974) 461–464.

[14] L.C. Yang, J. Appl. Phys. 45 (6) (1974) 461–464.

[15] J.D. O'Keefe, C.H. Skeen, Appl. Phys. Lett. 21 (10) (1972) 464–465.

[16] B.P. Fairand, A.H. Clauer, Opt. Comm. 18 (4) (1976) 588–591.

[17] R. Fabbro, J. Fournier, P. Ballard, D. Devaux, J. Virmont, J. Appl. Phys. 68 (2) (1990) 775–784.

[18] Zhang Hong, Ph.D.Dissertation, Nanjing University of Aeronautics and Astronautics, Nanjing, 1997, pp 1–103.

[19] J.W. Dally, W.F. Riley, Experimental Stress Analysis, McGraw-Hill, New York, 1978, pp. 76–81.

[20] A.H. Clauer, B.P. Fairand, B.A. Wilcox, Metall. Trans. A 8 (1977) 119–125.

[21] B.P. Fairand, A.H. Clauer, in: S.D. Ferris, H.J. Leony, J.M. Poate (Eds.), Laser-Solid Interactions and Laser Processing-1978, American Institute of Physics, New York, 1979, pp. 27–42.

[22] D.V. Nelson, Residual Stress Effects in Fatigue, ASTM STP 776, American Society for Testing Materials, 1982, pp. 172–194.